BHM Berg- und
Hüttenmännische
Monatshefte

Study on The Influence of the Blade on Powder Layers Built in Powder Bed Fusion Processes for Additive Manufacturing

Marco Mitterlehner, Herbert Danninger, Christian Gierl-Mayer, Johannes Frank, and Wolfgang Tomischko

Institut für Chemische Technologien und Analytik, TU Wien, Vienna, Austria

Abstract: For Additive Manufacturing (AM) performed by the laser powder bed fusion process, important aspects are not only powder characteristics such as flowability but also the morphology of the top layer itself. In the present study, the quality of the first applied top layer was studied using a self-made tester for the layer building process and a digital microscope with a large depth-of-field to observe the surface of the top layer. The three-dimensional images obtained have then been analyzed by a program, written by the corresponding author, that calculates specific parameters as well as the size of the particles in the top layer to rate the quality of the surface. Using this technique, the influence of using different blades and varying the blade speed during the layer building process on the quality of the surface has been investigated.

Keywords: Additive manufacturing, Powder bed fusion, Direct laser melting, Layer building tester, Powder layer morphology, Spreading, Blade, Testing, Python

Studie über den Einfluss der Beschichterklinge auf Pulverschichten in Pulverbettverfahren für die Additive Fertigung

Zusammenfassung: Wichtige Aspekte im Bereich der additiven Fertigung basierend auf der Laser-Pulverbetttechnologie sind zum Beispiel nicht nur die Pulvercharakteristika wie die Fließfähigkeit, sondern auch die Morphologie der obersten aufgetragenen Pulverschicht selbst. In dieser Studie wurde die Qualität der ersten aufgetragenen Pulverschicht analysiert. Dies erfolgte mit Hilfe eines selbst entwickelten Prüfgeräts zur genaueren Untersuchung der obersten aufgetragenen Schicht und eines Digitalmikroskops mit einer großen Tiefenschärfe, mit welchem die aufgetragene Schicht dreidimensional abgebildet werden kann. Die dreidimensionalen Aufnahmen wurden dann mittels eines selbst geschriebenen Python-Programms analysiert, welches eigens dafür entwickelte Parameter sowie die Größe der Partikel in der obersten Schicht berechnet, um so die Qualität einer aufgetragenen Schicht bewerten zu können. Unter Verwendung dieser Technologie wurde der Einfluss verschiedener Beschichterklingen bei Variation der Pulverauftragsgeschwindigkeit auf die Qualität der aufgetragenen Schicht untersucht.

Schlüsselwörter: Additive Fertigung, Pulverbettverfahren, Selektives Laser Schmelzen, Schichtbildung, Prüfgerät, Pulverschicht, Morphologie, Pulverauftrag, Beschichterklinge, Prüfgerät, Python

M. Mitterlehner (✉)
Institut für Chemische Technologien und Analytik,
TU Wien,
Getreidemarkt 9/164-CT,
1060 Vienna, Austria
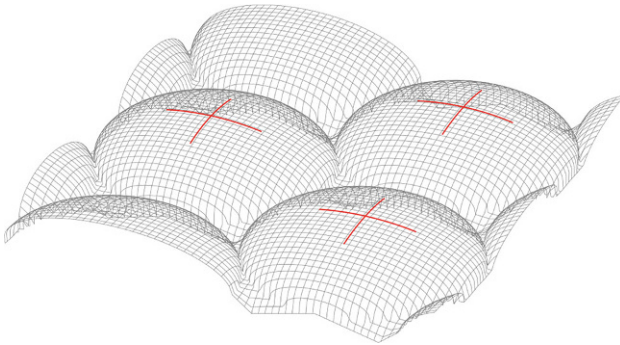marco.mitterlehner@tuwien.ac.at

1. Introduction

In the field of additive manufacturing techniques that use powder bed systems, several well-known powder characteristics, such as flowability or apparent density, are checked. Apart from these powder properties, new testing methods are also available [1–4]. Yet, during the building process, the quality, in particular the filling as well as the homogeneity, of the applied top powder layers is of crucial importance. Evaluating this, especially quantitatively, is of high practical relevance, even though it is a challenging task.

As described in [5–7], a new method for describing and rating the quality of the top spread layer using a powder bed system has been developed which is presented in short: The surface of the spread layer is investigated with a digital microscope taking three-dimensional images. These images are then analysed by a program, written by the corresponding author, which scans the surface in two directions (horizontal and vertical). That means, one line profile after the other in both directions is investigated, and the program searches for maxima occurring at the same location in both directions. Doing so, each of these maxima is equivalent to one particle in the surface, since this is a unique feature in this kind of surfaces, which can be used to rate the

Fig. 1: Unique maximum in both directions

quality of a spread layer. For better understanding, this is shown in Fig. 1, which also shows what a perfect surface in this case would look like consisting of exclusively spherical particles with the same size of the mass-median-diameter ($d_{3,50}$) and being packed most closely (hexagonal or cubic, both achieving the same packing density [8]).

Apart from this very specific method, another method has been developed for this study in which the density of just one single spread powder layer is evaluated.

2. Spreading

At the moment there are several SLM-printer providers and so there are several ways of spreading the powder during the process, which differ for example in the chronological order of the single process steps, the used blade, or some building parameters. Although all machines differ in their own way, the underlying process is always the same. Thereby, it is important to spread a dense powder layer in order to selectively melt enough material in the actual layer. Two aspects that are decisive for spreading dense layers are the distance between the blade and the building platform also called gap size (δ) and the layer thickness (d_l). Thus, in the first layer δ determines the layer thickness, and, in each further layer, it depends on the layer thickness if δ

still determines the layer thickness or not. After spreading the first layer and selectively melting the powder in it, the building platform is lowered and there are three different ways to do so with regard to the layer thickness, as shown in Fig. 2.

In Case 1 the layer thickness is lower than the distance between the blade and the building platform ($d_l < \delta$), resulting in the molten material protruding the initial level of the building platform. In Case 2 the layer thickness is equal to the distance between the blade and the building platform ($d_l = \delta$), resulting in the molten material being at the same level as the initial position of the building platform. In Case 3 the layer thickness is bigger than the distance between the blade and the building platform ($d_l > \delta$), resulting in the molten material being beneath the initial level of the building platform. Only in Case 2 a uniform process can be performed from the beginning to the end, which is why only Case 2 should be considered more closely.

From now on, to spread dense layers, δ is important as is d_l because, in case of a powder containing only spherical particles with the same size (D), no powder would remain on the building platform or rather on the molten material in the layer beneath if D were bigger than δ (Fig. 3a). That means, to spread dense layers, it is important that the distance between the blade and the building platform or subsequently the molten material beneath has to be bigger than the particles (Fig. 3b). In fact, powders used for SLM do not contain only particles with the same size but have a certain distribution, for which the $d_{3,50}$-value is a common characteristic value. Usually in SLM processes, the layer thickness (d_l) is around ~20 to 40 µm as is δ, but the particle size distribution ranges of the used powders are around ~15 to 63 µm, which means that most particles in the used powders are bigger than the distance between the blade and the building platform or rather the molten material in the layer beneath. This results, on the one hand, in a segregation of the powder every time the powder is spread over molten material or also in the area in front of the powder bed (Fig. 3c), whereby smaller particles remain on the molten material and bigger ones remain in the spread powder heap. On the other hand, empty spaces start to form in the spread layer on the
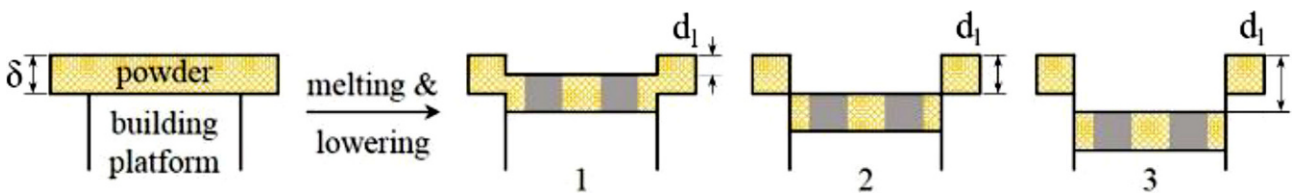

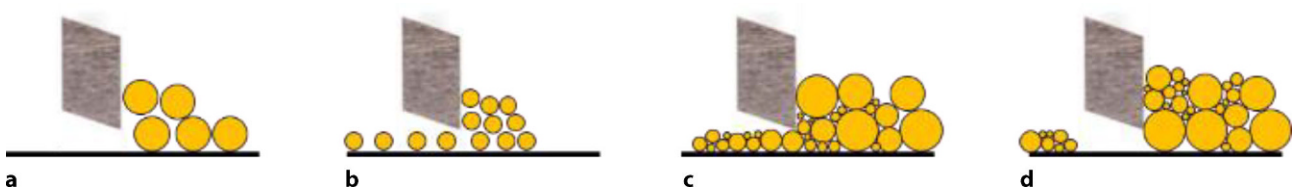
Fig. 2: Ways to lower the building platform

Fig. 3: Spreading scenarios (**a** too small gap size, **b** normal spreading behavior, **c** segregation, **d** formation of empty spots)
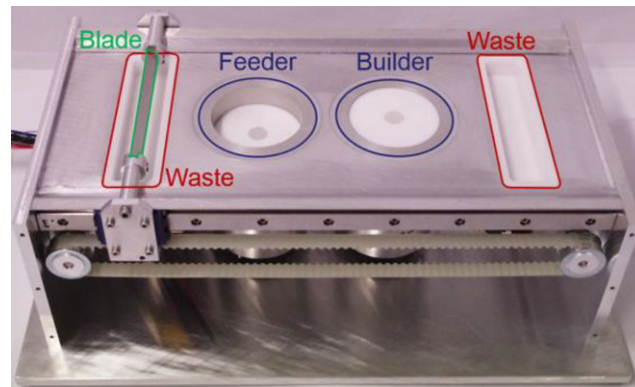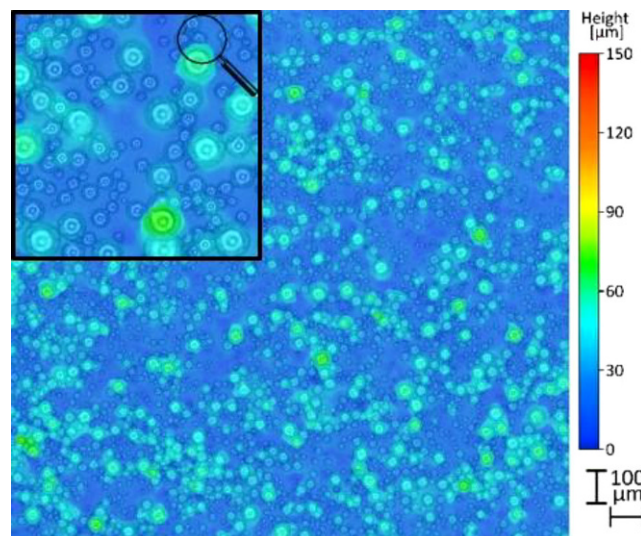
Fig. 4: Spreading tester


Fig. 5: Spread layer including empty spots

molten material (Fig. 3d) as simulated in [9]. Besides δ, another aspect that influences the presence of empty spaces is the velocity of the blade during spreading as is shown in the results.

3. Rating the Spread Layer

As shown in Fig. 4, a special tester has been developed to observe the surface of the top spread layer in SLM technologies. The so-called spreading tester can be controlled using a LabVIEW program written by the corresponding author, and parameters, such as the number of spread layers, used overspill of powder in the feeder or builder and layer thickness, and spreading velocity (v_{blade}), can be varied. Apart

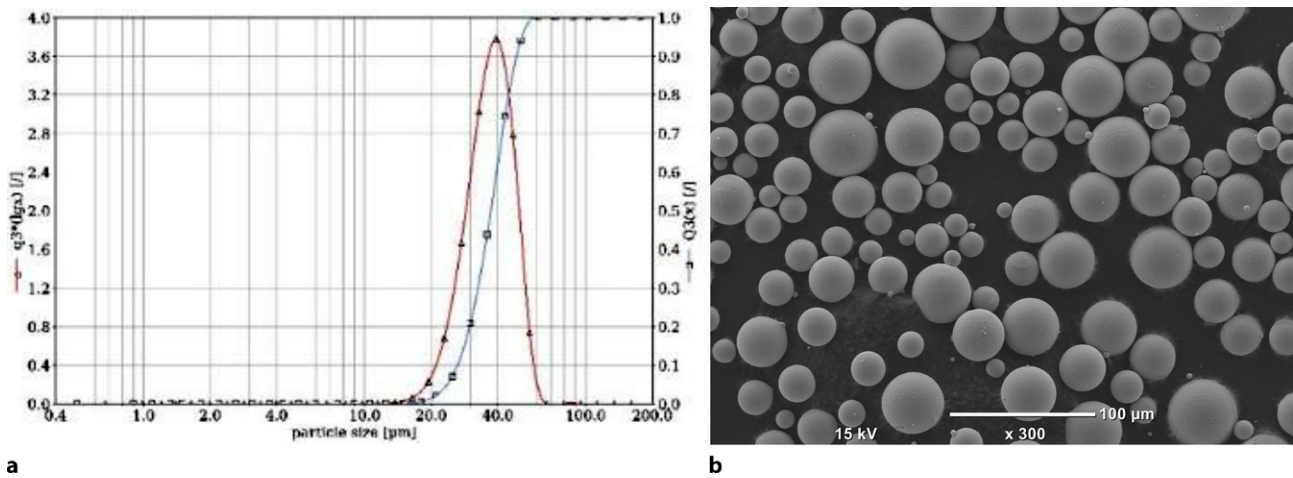Fig. 6: Height distribution of the spread layer from Fig. 5

a

b
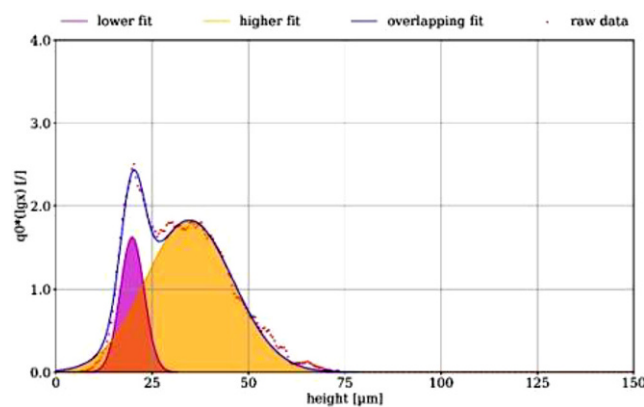
Fig. 7: Particle size distribution (**a**) and SEM image (**b**, 300× magnified)

from these basic parameters, the mimicked machine can be changed. At the moment the layer building procedure of an EOS M280 or a Concept Laser M1 machine can be chosen.

Next to these software parameters, hardware parameters, like the distance between the blade and the building platform—also called gap size (δ)—the angle of the blade or even the blade itself, can be varied so that high speed steel blades as well as different kinds of polymer blades can be used.

Evaluating the density of a spread layer afterwards is then performed by analysing the formation of empty spots as mentioned before. Therefore, just one layer is spread on the building platform of the spreading tester, which is roughly equivalent to spreading on already molten material. Then three-dimensional images of the surface are made which may contain empty spots as seen in Fig. 5 using a digital microscope. Now, in order to determine the amount of empty space (ψ) between the powder particles, the height distribution of the entire surface is plotted, which can be seen in Fig. 6. This clearly shows the appearance of two peaks, which are then fitted by using Gaussian curves. Thereby the lower one (purple) can be assigned to the empty spaces and the upper one (orange) can be assigned to the particles in the surface. Taking a closer look at

the magnified area in Fig. 5, it can be seen that the software of the used digital microscope somehow smoothens the surface, since the area right next to the particles is not dark blue as it should be, which would indicate that the height at this position would be zero. This means that the height of the building platform is not always zero but somehow distributed in the range of a few microns, which explains why the lower peak can be assigned to the building platform. Then the amount of the area beneath the lower fitted peak with respect to the total area beneath all fitted peaks is calculated which is equivalent to the amount of empty space.

4. Powder Used and Its Characteristics

In this study a gas atomized and afterwards plasma spheroidized Ni-based alloy powder (L718, voestalpine Böhler Edelstahl GmbH & Co KG, Austria) has been used. The PSD measured using laser diffraction by a Sympatec HELOS/BF system is shown in Fig. 7a. It can be seen that the distribution is tight and uniform and that the powder contains particles from 15 to 65 µm with a $d_{3,\,50}$-value of 36.44 µm.

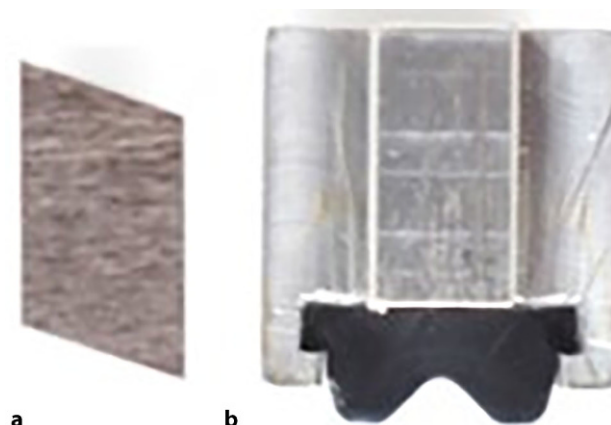**Fig. 8:** HSS blade (**a**) and polymer blade (**b**)

a   **b**

The powder has also been investigated by scanning electron microscopy (JEOL JCM-6000), as shown in Fig. 7b. As can be seen, the particles in the powder are very spherical and there are no agglomerates or satellites.

The flowability using a Hall Funnel, the apparent density (using a Hall Funnel due to the fact that the powder was flowing freely), and the apparent density using an Arnold Meter have been determined as well. For each powder characteristic, three individual measurements have been carried out and then an arithmetic mean value as well as the standard deviation have been calculated. As mentioned above the powder flows freely with a good flowability of $10.81 \pm 0.11\,\text{s}/50\,\text{g}$. The apparent density measured by the Hall Funnel is $4.61 \pm 0.01\,\text{g/cm}^3$ and the one measured by the Arnold Meter is slightly higher due to the different type of measurement and is $4.81 \pm 0.01\,\text{g/cm}^3$.

5. Testing of the Spread Layer

In this study, an EOS M280 machine has been mimicked using two different kinds of blades: one HSS blade (Fig. 8a) and one polymer blade (Fig. 8b). Now to investigate different influences on the amount of empty space, only one layer has been spread, whereby the gap size (δ) as well as the velocity of the blade during spreading (v_{blade}) has been varied. For each blade, experiments have been carried out with δ being 30, 50, 60, and 80 µm and v_{blade} being 50, 100, 200, 300, and 400 mm/s.

After the layer building process, the builder is removed from the tester in order to place under the digital microscope and to take three-dimensional images. This has always been done carefully in order to avoid changing the morphology of the top layer.

The images have been made using a Keyence VHX 5000 digital microscope at a magnification of 800×. One image is

Fig. 10: Amount of empty space of the HSS blade (*left bars*) and the polymer blade (*right bars*) as a function of the gap size (δ)
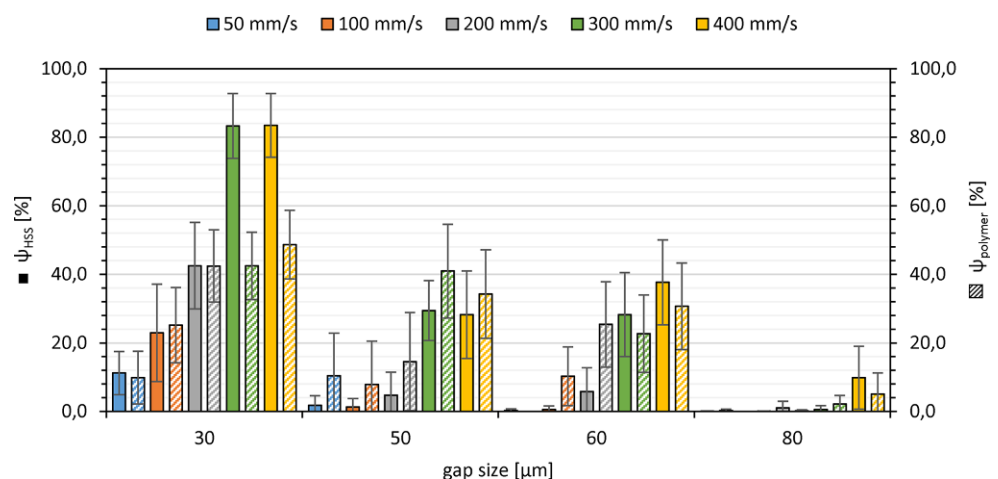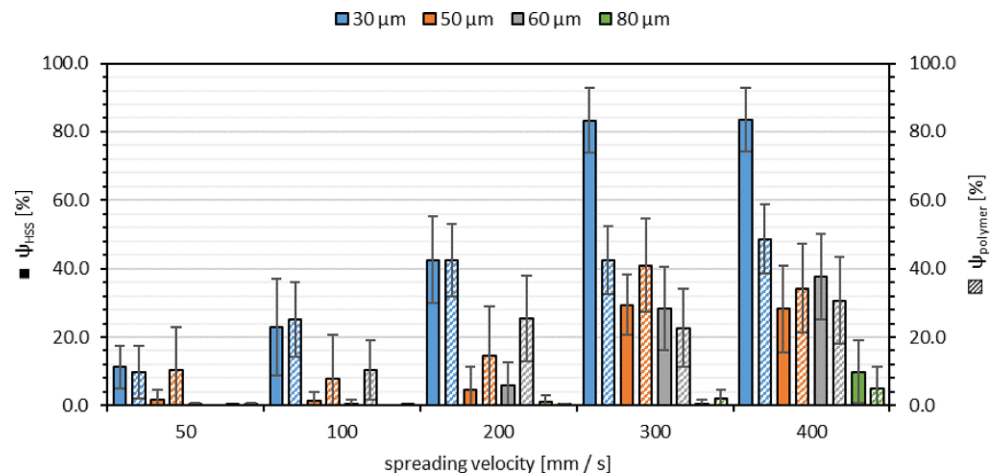
stitched together from 30 single images and has the size of about ~1.1 × 1.1 mm. For every surface, images have been taken from 9 different spots, as seen in Fig. 9.

6. Results and Discussion

In Fig. 10 the amount of empty space (ψ) as a function of the gap size (δ) is shown, whereby the solid bars depict ψ of the HSS blade and the hatched bars depict ψ of the polymer blade. Thereby, it is important to say that the relatively high scatter is caused by the building platform, which is not perfectly parallel to the blade. Yet, since the building platform was never moved during all these experiments, it was always in the same position.

Taking a closer look at Fig. 10, it can be seen that, when comparing the different blades, similar trends can be observed. Overall it is easy to see that, for a constant gap size, the amount of empty space always increases as the spreading velocity increases. This probably happens because the particles are accelerated too much and so they are not able to remain in a dense layer.

In case of a gap size of 80 μm, which is approx. 2.2 times the $d_{3, 50}$-value, it is possible to spread almost dense layers even with a maximum spreading velocity of 300 mm/s, since the biggest particles in the used powder have a size of around 65 μm. Nevertheless, when using a spreading velocity of 400 mm/s, the influence of the spreading velocity outweighs the influence of the gap size and no dense layer could be spread.

In case of a 50 and 60 μm gap size, which would be approx. 1.4 and 1.6 times the $d_{3, 50}$-value, it was possible to spread fairly dense layers up to a maximum spreading velocity of 100 mm/s but only when using the HSS blade. When using the polymer blade, fairly dense layers could only be applied by using the 60 μm gap size and a maximum of 100 mm/s spreading velocity.

In case of the 30 μm gap size, which is approx. 0.8 times and therefore smaller than the $d_{3, 50}$-value, no dense layers could be spread regardless of the used blade, due to the fact that the gap size is too small for most particles to pass through. When using the 30 μm gap size, also the highest

difference in ψ between the two blades is observed when looking at high spreading velocities of ≤300 mm/s, whereby the HSS blade creates significantly more empty spaces than the polymer blade.

In Fig. 11 the amount of empty space (ψ) as a function of the spreading velocity (v_{blade}) is shown, whereby again the solid bars depict ψ of the HSS blade and the hatched bars depict ψ of the polymer blade. Thereby, it can be seen that the amount of empty space always decreases as the gap size increases while the spreading velocity is constant. This is due to the fact that the gap size gets bigger and so more particles are able to pass through.

7. Summary

In this study, the procedure to characterize a spread layer as described in [5–7] has been extended by the development of a new method to quantify the presence of empty spots in spread layers.

Furthermore, the influence of the distance between the blade and the building platform or rather the molten material in the layer beneath (gap size) as well as the spreading velocity on the fraction of empty space in the spread layer were investigated. Thereby, independently of the used blade, it was observed that the higher the gap size and the lower the spreading velocity was, the lower the amount of empty space in the spread layer. Additionally, it could be shown that, with a gap size of ~1.5 times the $d_{3, 50}$-value, almost dense layers can be spread at low spreading velocities (e.g. 50 or 100 mm/s). Considering the fact that the gap size is equal to the layer thickness, this would mean that the higher the layer thickness, the denser the spread surface (this statement, however, should be taken with caution regarding the effect of layer thickness on layer building).

Pronounced differences between the two used blades could only be observed while using the smallest gap size (30 μm) and the highest spreading velocities (300 and 400 mm/s) as well as the parameters when starting to spread almost dense layers (HSS blade 50 μm and polymer blade 60 μm).

References

1. RETSCH Technology GmbH: Determination of Particle Shape with Dynamic Image Analysis, AZoM, 2019 https://www.azom.com/article.aspx? ArticleID=17328 (17 May 2019)
2. Lumayabd, G.; Boschiniac, F.; Trainaac, K.; Bontempia, S.; Remyb, J.-C.; Clootsac, R., Vandewalleab, N.: Measuring the flowing properties of powders and grains, Powder Technology, 224 (2012), pp 19–27
3. Methods for Powder and Granular Media Characterization with the Anton Paar Powder Cell, Anton Paar, https://www.anton-paar.com/corp-en/services-support/document-finder/application-reports/methods-for-powder-and-granular-media-characterization-with-the-anton-paar-powder-cell/ (17 May 2019)
4. Hare, C.; Zafar, U.; Ghadiri, M.; Freeman, T.; Clayton, J.; Murtagh, M.: Analysis of the Dynamics of the FT4 Powder Rheometer, Powder Technology, 285 (2015), pp 123–127
5. Mitterlehner, M.; Danninger, H.; Gierl-Mayer. C.: A New Method For Describing The Morphology Of Powder Layers In Direct Laser Melting, Proceedings of the 3rd Metal Additive Manufacturing Conference, Austrian Society for Metallurgy and Materials (ASMET), Vienna, 2018, pp 31–40
6. Mitterlehner, M.; Danninger, H.; Gierl-Mayer. C.: Study On The Layer Building Of Powders In Powder Bed Fusion Processes For Additive Manufacturing, Proceedings of the Euro PM2018 Congress & Exhibition, Bilbao, 2018, Paper-Nr. 3988826
7. Mitterlehner, M.; Danninger, H.; Gierl-Mayer. C.: Study On Segregation Effects in Powder Layers Built In Powder Bed Fusion Processes For Additive Manufacturing, Proceedings of the Euro PM2019 Congress & Exhibition, Maastricht, 2019, Paper-Nr. 4346412
8. Chang, H.-C.; Wang, L.-C.: A Simple Proof of Thue's Theorem on Circle Packing, L'Enseignement Mathématique, 38 (2010), pp 125–131
9. Nan, W.; Pasha, M.; Bonakdar, T.; Lopez, A.; Zafar, U., Nadimi, S.; Ghadiri, M.: Jamming during particle spreading in additive manufacturing, In: Powder Technology, 338 (2018), pp 253–262